DOI: 10.1002/jcc.21883

Comparison Between Self-Guided Langevin Dynamics and Molecular Dynamics Simulations for Structure Refinement of Protein Loop Conformations

Mark A. Olson,*[a] Sidhartha Chaudhury,[b] and Michael S. Lee[a,c]

This article presents a comparative analysis of two replica-exchange simulation methods for the structure refinement of protein loop conformations, starting from low-resolution predictions. The methods are self-guided Langevin dynamics (SGLD) and molecular dynamics (MD) with a Nosé–Hoover thermostat. We investigated a small dataset of 8- and 12-residue loops, with the shorter loops placed initially from a coarse-grained lattice model and the longer loops from an enumeration assembly method (the Loopy program). The CHARMM22 + CMAP force field with a generalized Born implicit solvent model (molecular-surface parameterized GBSW2) was used to explore conformational space. We also assessed two empirical scoring methods to detect nativelike conformations from decoys: the all-atom distance-scaled ideal-gas reference state (DFIRE-AA) statistical potential and the Rosetta energy function. Among the eight-residue loop targets, SGLD out performed MD in all cases, with a median of 0.48 Å reduction in global root-mean-square deviation (RMSD) of the loop backbone coordinates from the native structure. Among the more challenging 12-residue loop targets, SGLD improved the prediction accuracy over MD by a median of 1.31 Å, representing a substantial improvement. The overall median RMSD for SGLD simulations of 12-residue loops was 0.91 Å, yielding refinement of a median 2.70 Å from initial loop placement. Results from DFIRE-AA and the Rosetta model applied to rescoring conformations failed to improve the overall detection calculated from the CHARMM force field. We illustrate the advantage of SGLD over the MD simulation model by presenting potential-energy landscapes for several loop predictions. Our results demonstrate that SGLD significantly outperforms traditional MD in the generation and populating of nativelike loop conformations and that the CHARMM force field performs comparably to other empirical force fields in identifying these conformations from the resulting ensembles. Published 2011 Wiley Periodicals, Inc.† J Comput Chem 00: 000–000, 2011

Keywords: comparative protein models · protein variable regions · conformational sampling · replica-exchange methods

Introduction

Refinement of comparative protein structures is of significant interest given the rapid decoding of new sequences from large-scale genomic efforts and the desire to model three-dimensional protein structures to accurate resolution. Notable examples of computational refinement of protein models include the work of Levitt and coworkers,[1–3] the work of the Baker lab[4–6] and Zhu et al.,[7] the work from the Skolnick group,[8,9] Jacobson and coworkers,[10] and Chen and Brooks,[11] among others that participated in recent Critical Assessment of Protein Structure Prediction meetings.[12] An integral component of structure refinement is the modeling of protein loops. One of the more exigent issues is how to improve the conformational sampling of all-atom simulation methods to "funnel" structures to the native loop basin on a vast energy landscape starting from low-resolution model predictions. A second issue is the development of scoring functions to detect the native conformation among a large set of loop decoys.

Molecular dynamics (MD) simulations for conformational sampling have often been employed for final-stage refinement of a predicted structure with promising results.[2,11–13] The most significant challenge to MD-based structure refinement is that the energy landscape of protein conformational space contains many potential-energy barriers that present kinetic traps to finding the native basin. One method designed to address this is temperature-based replica exchange (T-ReX),[14] which uses multiple parallel simulations at a range of temperatures to overcome local minima and promote large conformational excursions along the potential-energy surface. Although T-Rex is frequently used with MD simulations and has enjoyed some success in structure refinement, it is often insufficient, particularly when refining longer loops or more complex systems. An alternative to MD, yet relatively untested method for improving

---

[a] *M. A. Olson, M. S. Lee*
Department of Cell Biology and Biochemistry, US Army Medical Research Institute of Infectious Diseases, Fredrick, Maryland 21702
E-mail: molson@compbiophys.org

[b] *S. Chaudhury*
Telemedicine and Advanced Technology Research Center, US Army Medical Research and Materiel Command, Biotechnology High Performance Computing Software Applications Institute, Frederick, Maryland 21702

[c] *M. S. Lee*
Computational Sciences and Engineering Branch, US Army Research Laboratory, APG, Maryland 21005

Contract/grant sponsor: US DoD Threat Reduction Agency; Contract/grant number: DTRA TMTI0004_09_BH_T; Contract/grant sponsor: Department of Defense Biotechnology High Performance Computing Software Applications Institute.

†This article is a US Government work and, as such, is in the public domain in the United States of America.

Report Documentation Page	*Form Approved* *OMB No. 0704-0188*

Public reporting burden for the collection of information is estimated to average 1 hour per response, including the time for reviewing instructions, searching existing data sources, gathering and maintaining the data needed, and completing and reviewing the collection of information. Send comments regarding this burden estimate or any other aspect of this collection of information, including suggestions for reducing this burden, to Washington Headquarters Services, Directorate for Information Operations and Reports, 1215 Jefferson Davis Highway, Suite 1204, Arlington VA 22202-4302. Respondents should be aware that notwithstanding any other provision of law, no person shall be subject to a penalty for failing to comply with a collection of information if it does not display a currently valid OMB control number.

1. REPORT DATE **2011**	2. REPORT TYPE	3. DATES COVERED **00-00-2011 to 00-00-2011**

4. TITLE AND SUBTITLE **Comparison Between Self-Guided Langevin Dynamics and Molecular Dynamics Simulations for Structure Refinement of Protein Loop Conformations**	5a. CONTRACT NUMBER 5b. GRANT NUMBER 5c. PROGRAM ELEMENT NUMBER
6. AUTHOR(S)	5d. PROJECT NUMBER 5e. TASK NUMBER 5f. WORK UNIT NUMBER
7. PERFORMING ORGANIZATION NAME(S) AND ADDRESS(ES) **U.S. Army Medical Research and Materiel Command,Biotechnology High Performance Computing Software Applications Institute,Telemedicine and Advanced Technology Research Center,Fort Detrick,MD,21702**	8. PERFORMING ORGANIZATION REPORT NUMBER
9. SPONSORING/MONITORING AGENCY NAME(S) AND ADDRESS(ES)	10. SPONSOR/MONITOR’S ACRONYM(S) 11. SPONSOR/MONITOR’S REPORT NUMBER(S)

12. DISTRIBUTION/AVAILABILITY STATEMENT
Approved for public release; distribution unlimited

13. SUPPLEMENTARY NOTES

14. ABSTRACT

15. SUBJECT TERMS

16. SECURITY CLASSIFICATION OF:			17. LIMITATION OF ABSTRACT	18. NUMBER OF PAGES	19a. NAME OF RESPONSIBLE PERSON
a. REPORT **unclassified**	b. ABSTRACT **unclassified**	c. THIS PAGE **unclassified**	**Same as Report (SAR)**	**9**	

Standard Form 298 (Rev. 8-98)
Prescribed by ANSI Std Z39-18

sampling is based on self-guided Langevin dynamics (SGLD) simulations.[15] The SGLD method differs from the standard Langevin equation by an introduction of *ad hoc* guiding force. This force term is calculated as a local average of the friction forces during a SGLD simulation and is thought to accelerate low-frequency modes that hinder transitions across high potential-energy barriers. Wu and Brooks demonstrated through several model systems that the SGLD simulation method can provide enhanced conformational sampling of an energy surface without significant alteration in conformational distribution.[15]

In this work, we seek to combine SGLD with T-ReX for the structure refinement of loops. Our goal is not to provide an exhaustive benchmarking of the SGLD/T-ReX method, but rather to contrast its performance with that of the more conventional MD/T-ReX simulations using a small dataset of loop targets. This dataset contains eight-residue loops, which are relatively tractable refinement problem for a number of loop modeling algorithms, and longer 12-residue loops, which are almost universally challenging for structure prediction and refinement.[16]

In addition to exploring the SGLD method, we also revisit the problem of detection of nativelike structures among decoys[17] by evaluating three scoring methods. The first is based on the force field and generalized Born implicit solvent model used to generate the loop conformations. The second approach is rescoring the conformations by the all-atom distance-scaled ideal-gas reference state (DFIRE-AA) statistical potential function.[18] The third approach is the Rosetta all-atom energy function.[19] In our study, side chains in the loop stem are modeled to be flexible during the simulations and thus replicate the inexact local environments found in real-world refinement of comparative protein models. Using the Rosetta method, we examine the possible benefit of repacking all side chains and their energy optimization. Motivation for applying the latter scoring method is the observation from previous studies that all-atom stimulations typically generate nativelike backbone conformations, yet placement of the side chains from thermal sampling often leads to a poorly defined energy funnel to the native basin.[20]

Computational Methods

Simulation models

As detailed by Wu and Brooks,[15] the scheme of self-guided simulations is to enhance conformational sampling by incorporating information extracted from the trajectory during the simulation. The information is typically a local property averaged over the adjoining protein conformational space near the current conformation of the simulation trajectory. An earlier development of this idea is self-guided MD simulations,[21] where time-averaged forces are applied as a guiding term. For the SGLD, time-averaged momentum is applied and has the effect of accelerating low-frequency modes. The equation of motion for an SGLD simulation is

$$\dot{\mathbf{p}}_i = \mathbf{f}_i - \gamma_i \mathbf{p}_i + \mathbf{R}_i + \lambda \mathbf{g}_i, \tag{1}$$

where $\dot{\mathbf{p}}_i$ is the rate of change of the momentum of particle *i*, $\mathbf{f}_i$ is the force acting on the particle, γ_i is the friction constant, $\mathbf{R}_i$ denotes the random force, and $\mathbf{g}_i$ is a memory function, which is scaled by guiding factor λ. The memory function $\mathbf{g}_i$ is defined by the moving average of the momentum seen by the system over an interval of time, L:

$$\mathbf{g}_i = \langle \mathbf{p}_i \rangle_L, \tag{2}$$

where $\langle \cdots \rangle_L$ denotes a local average. The time interval is further defined as $L = t_L/\delta t$, where t_L is the local averaging time and δt the time step along the simulation trajectory. Equation (2) indicates that the guiding force is a local average of the friction force and should increase the chances of sampling the native or lowest energy topology of a protein by preferentially increasing the speed of the slowest conformational motions. However, as noted by Wu and Brooks, the SGLD equation of motion is fundamentally approximate. This approximate nature was investigated in a recent study of the SGLD method used to model protein folding–unfolding transitions and it was observed that the main drawback of incorporating the *ad hoc* force term is possible distortion of the free-energy surface applied to the calculation of thermodynamic observables.[22] Here, we investigate the applicability of the SGLD method to model conformational changes that are inherently much smaller than protein folding and whether the method can do so without incurring significant distortions in the distribution of potential energies.

Our SGLD model simulations were carried out using the CHARMM22 force field with the CMAP backbone dihedral cross-term extension.[23,24] The friction constant γ was set to 1 ps^{-1} for all heavy atoms, the guiding factor λ set to a value of 1, and the averaging time t_L was set to 1 ps. Selection of these values was taken from our previous study of the SGLD model.[22] For comparison purposes, MD simulations were applied using a Nosé–Hoover thermostat with a temperature coupling constant of 50 kcal s^{-2}. An integration time step of 2 fs was used for all simulations. Nonbonded interaction cutoff parameters for electrostatics and vdW terms were set at a radius of 22 Å with a 2-Å potential switching function. Covalent bonds between the heavy atoms and hydrogens were constrained by the SHAKE algorithm.[25] For modeling the protein stem outside of the loop segment and to prevent unfolding at higher temperatures, C_α and C_β atom coordinates were tethered to their initial crystallographic positions with a force constant of 1.0 kcal (mol^{-1} Å^{-2}).

To model electrostatic solvent effects, we used the molecular-surface-based generalized Born switching-window (GBSW2) solvent model.[26] This implicit solvent model was parameterized to fit the Lee–Richards molecular-surface Poisson results and requires model parameters to be set to values of $w = 0.2$ Å, $a_0 = 1.2045$, and $a_1 = 0.1866$. The hydrophobic cavitation energy term was approximated by a linear product of the solvent-exposed surface area of the solute and a phenomenological surface tension coefficient set to 30 cal (mol^{-1} Å^{-2}).

The application of the GBSW2 model is in contrast to the earlier calculations where the GBMV2 implicit solvent model was used.[20] This revision in our simulation approach has several potential advantages. It has been shown by Chocholoušová and Feig[26] that GBSW2 exhibits good agreement with Poisson calculated solvent energies and, because of the existence of fewer higher frequency components in the GBSW2 model as compared with GBMV2, the protein–solvent dielectric transition is less abrupt. The advantage of improved smoothness of the dielectric boundary should allow greater excursions on rugged conformational energy landscapes by increasing transmission probabilities across high potential-energy barriers. In addition, more stringent energy conservation should be obtained by GBSW2 using the Nosé–Hoover and Langevin thermostats, and subsequently yield improvement in sampling convergence.[26] As a practical note, GBSW2 is more computationally efficient than GBMV2 due to the calculational scheme of determining the Born radii. Despite these advantages, one possible shortcoming of GBSW2 compared with GBMV2 is the introduction of artifacts in conformational landscapes computed for thermodynamic protein folding.[27] While this disadvantage may have an effect in some cases of structure refinement, where large perturbations are required of the nature of unfolding–folding transitions, it is most probably negligible for modeling medium size loops.

Replica-exchange simulations were performed using the MMTSB[28] utilities and programming libraries for implementing the CHARMM simulation program (version c33b2).[29] Simulations were carried out over a total of 4-ns simulation time for each replica, generating a final culled population of 64,000 loop conformations for each loop target using 16 replicas with the temperature range of 298–400 K. Frequency of replica exchanges was set to every 1 ps of simulation. The starting input structures for the protein targets into the T-ReX simulations were obtained from two different methods. For modeling eight-residue loops, the starting structures were generated from a low-resolution cubic lattice model and details of the simulation protocol are given in earlier work.[20] Initial placement of 12-residue loop coordinates is based on predictions using the enumeration scheme of the Loopy program developed by the Honig lab.[30] The top-scoring structure from Loopy is used as input to SGLD and MD simulations to search conformational space of locating more optimal loop conformations. Our test set consists of five 8-residue loops and six 12-residue loops taken from a diverse set of protein structures.[16,30]

Scoring of protein structures

Three different scoring functions were applied to select the "best" loop conformation from the ensemble of conformers generated by the simulation models. The first is identical to the force field (CHARMM22 + CMAP with the GBSW2 model) used to generate the loop decoys. Here, we define the scoring function as

$$G = U_{\mathrm{int}} + G_{\mathrm{solv}} - \mathrm{k_B} T \ln M, \tag{3}$$

where each loop conformation is evaluated as the sum of the internal potential energy, U_{int}, and the GBSW2 solvent energy, G_{solv}, plus a term that accounts for the multiplicity of conformations,[20] M, for a cluster of loop structures at absolute temperature T, and where k_B is the Boltzmann constant. Culled conformations from the T-ReX simulations were clustered on the basis of pairwise backbone root-mean-square deviation (RMSD) distances (described below). A hierarchical clustering scheme was applied that includes an agglomerative approach with automatic stopping criteria. Specific details of our clustering approximation are given in previous work.[20]

In addition to culling structures at the specific temperature of 298 K from T-ReX for direct scoring using eq. (3), we used the weighted histogram analysis method (WHAM)[31] to calculate the probability density of conformational states as a function of the total conformation energy ($U_{\mathrm{int}} + G_{\mathrm{solv}}$) and RMSD from the X-ray crystallographic structure. In our WHAM calculations, conformations from all 16 replicas were applied and we report free energies calculated for $T = 298$ K.

The second energy scoring function is the DFIRE-AA statistical potential[18] and is defined as

$$E_{\mathrm{DFIRE}}(i,j,r) = -\mathrm{k_B} T \ln \left[\frac{N_{obs}(i,j,r)}{\left(\frac{r}{r_{cut}}\right)^{\alpha} \frac{\Delta r}{\Delta r_{cut}} N_{obs}(i,j,r_{cut})} \right], \tag{4}$$

where i and j are non-hydrogen atom types, r is a pairwise distance, r_{cut} is the cutoff beyond which pairwise interactions are neglected, Δr is the histogram bin size, N_{obs} is a cumulative histogram of the observed occurrence of pairs as a function of the pairwise distance, and α is set to 1.61 based on an empirical analysis of hard-sphere protein-like spatial distributions. The histograms N_{obs} in this work were obtained from previous analysis of a culled set of 1836 Protein Data Bank (PDB) structures which had better than 1.8-Å resolution and were less than 30% homologous to each other.[17] We deviated from the original DFIRE protocol by assigning $\Delta r = 0.5$ Å at all distances and having r range from 0.25 to 14.75 Å, such that $r_{\mathrm{cut}} = 15$ Å.

The third scoring approach is application of the Rosetta energy function. The challenge in using the Rosetta energy function to score loop decoys selected from a 298-K ensemble generated from the CHARMM22 + CMAP/GBSW2 force field is that they are suboptimal structures under the Rosetta energy function. Our general approach is twofold: first, to improve suboptimal structures in CHARMM-generated in Rosetta by allowing limited sampling to identify a local minimum in the Rosetta energy landscape near a given decoy structure; second, to modify the Rosetta energy function to accommodate suboptimal structural features that cannot be improved by the limited sampling. Toward these ends, we developed a simple protocol using Rosetta v3.1[19] that optimizes hydrogen placement, packs side chains, and minimizes and calculates the energy under a modified Rosetta energy function.

For each decoy, the following protocol was followed. First, we used Rosetta to replace hydrogen atoms using standard bond geometry derived from the CHARMM19 force field.[32] We then used the Rosetta fixed-backbone packing application[33] to optimize the decoy side-chain conformations under the Rosetta energy function using the backbone-dependant rotamer library developed by Dunbrack and Cohen[34] that was expanded to include rotamers at ±1 standard deviation from the standard χ values at χ_1 and χ_2,[35] as well as extra rotamers

Table 1. Structure refinement of loop conformations using replica-exchange MD and SGLD simulations

Model	Starting loop RMSD	% Loops sampled RMSD < 2 Å	Lowest sampled RMSD	Force-field detection RMSD	DFIRE-AA scoring RMSD	Rosetta scoring RMSD
8-Residue loops						
1lit:82–89	2.21					
MD		24	0.87	1.92	2.23	5.03
SGLD		67	1.19	1.44	2.18	1.48
1plc:6–13	4.58					
MD		18	0.56	7.30	7.92	7.07
SGLD		68	0.44	0.66	0.79	0.52
1awd:56–63	3.61					
MD		99	0.27	0.79	0.52	0.61
SGLD		100	0.26	0.68	0.63	0.45
1hfc:119–126	3.09					
MD		99	0.33	1.01	0.61	0.73
SGLD		95	0.35	0.80	0.96	0.87
1rro:18–25	2.31					
MD		84	0.44	1.39	0.81	0.78
SGLD		82	0.46	0.63	1.12	0.85
12-Residue loops						
1bkf:9–20	2.70					
MD		21	1.37	2.43	2.46	1.98
SGLD		34	0.37	0.88	2.45	2.16
1ayh:21–32	4.30					
MD		0	1.91	4.55	4.35	2.74
SGLD		6	1.22	2.64	1.27	2.63
1cex:23–34	1.50					
MD		100	0.38	0.82	0.68	0.59
SGLD		100	0.40	0.62	0.61	0.63
1akz:181–192	2.20					
MD		<1	1.89	3.12	2.93	1.99
SGLD		0	2.24	3.83	2.97	2.68
153l:98–109	2.80					
MD		84	1.08	1.66	1.83	1.81
SGLD		89	0.36	0.86	1.96	1.33
1arb:74–85	2.70					
MD		25	1.17	2.00	1.99	2.14
SGLD		88	0.61	0.93	0.67	0.85

All RMSD values are in units of Angstrom.

at χ_3 and χ_4.[36] The initial decoy side-chain conformations were also added to the library. Following packing, the structure was energy minimized along backbone and side-chain torsion angles using a gradient-based single-line minimization scheme and scored under the Rosetta energy function, using the scoring application in Rosetta v3.1.

The Rosetta energy function, E_{Rosetta}, consists of a linear combination of energy terms that represent van der Waals interactions, residue–residue interactions, solvation, hydrogen-bonding, and side-chain and backbone conformational energies:

$$\begin{aligned} E_{\text{Rosetta}} &= 0.8E_{\text{LJattr}} + 0.44E_{\text{LJrep}} + 0.49E_{\text{pair}} + 0.65E_{\text{solv}} \\ &+ 0.58E_{\text{HB-short(bb-bb)}} + 1.17E_{\text{HB-long(bb-bb)}} + 1.17E_{\text{HB(bb-sc)}} \\ &+ E_{\text{HB(sc-sc)}} + 0.56E_{\text{rot}(\text{aa},\varphi,\psi)} + 0.2E_{\varphi,\psi(\text{aa})} + E_{\text{aa}(\varphi,\psi)}, \end{aligned} \tag{5}$$

where van der Waals interactions are represented by the attractive and repulsive parts of a modified 12-6 Lennard–Jones potential (E_{LJattr}, E_{LJrep}). Residue–residue interactions are modeled using a residue pairwise potential (E_{pair}) derived from PDB statistics. Solvation is modeled using the Lazaridis–Karplus implicit solvation model (E_{solv}).[37] Hydrogen-bonding is modeled using an orientation-dependent potential parameterized from quantum mechanics calculations[38] and PDB statistics[39] for short-range (bond length $<$ 2.6 Å) and long-range (bond length $>$ 2.6 Å) backbone–backbone hydrogen bonds ($E_{\text{HB-short(bb–bb)}}$, $E_{\text{HB-long(bb–bb)}}$), backbone–side-chain hydrogen bonds ($E_{\text{HB(bb–sc)}}$), and side-chain–side-chain hydrogen bonds ($E_{\text{HB(sc-sc)}}$).[40] Side-chain and backbone conformational energies are represented by statistical potentials derived from amino-acid and backbone-dependent rotamer probabilities ($E_{\text{rot}(\text{aa},\varphi,\psi)}$), amino-acid-dependent φ/ψ angle probabilities ($E_{\varphi,\psi(\text{aa})}$), and φ/ψ angle-dependent amino-acid probabilities ($E_{\text{aa}(\varphi,\psi)}$), derived from PDB statistics.[35,36,40]

Weights of the individual terms in eq. (5) were obtained from an updated and modified version of score12, the weight-set originally used for all-atom structural refinement.[5] Compared with the standard score12 weight-set,[19] we removed the "pro_close" and "omega" energy terms, which are statistical potentials reflecting proline-ring strain energy and backbone ω torsional energy. Near-native structures generated under the CHARMM force field showed high energies along these statistical energy terms compared with crystal structures, which significantly impeded decoy discrimination.

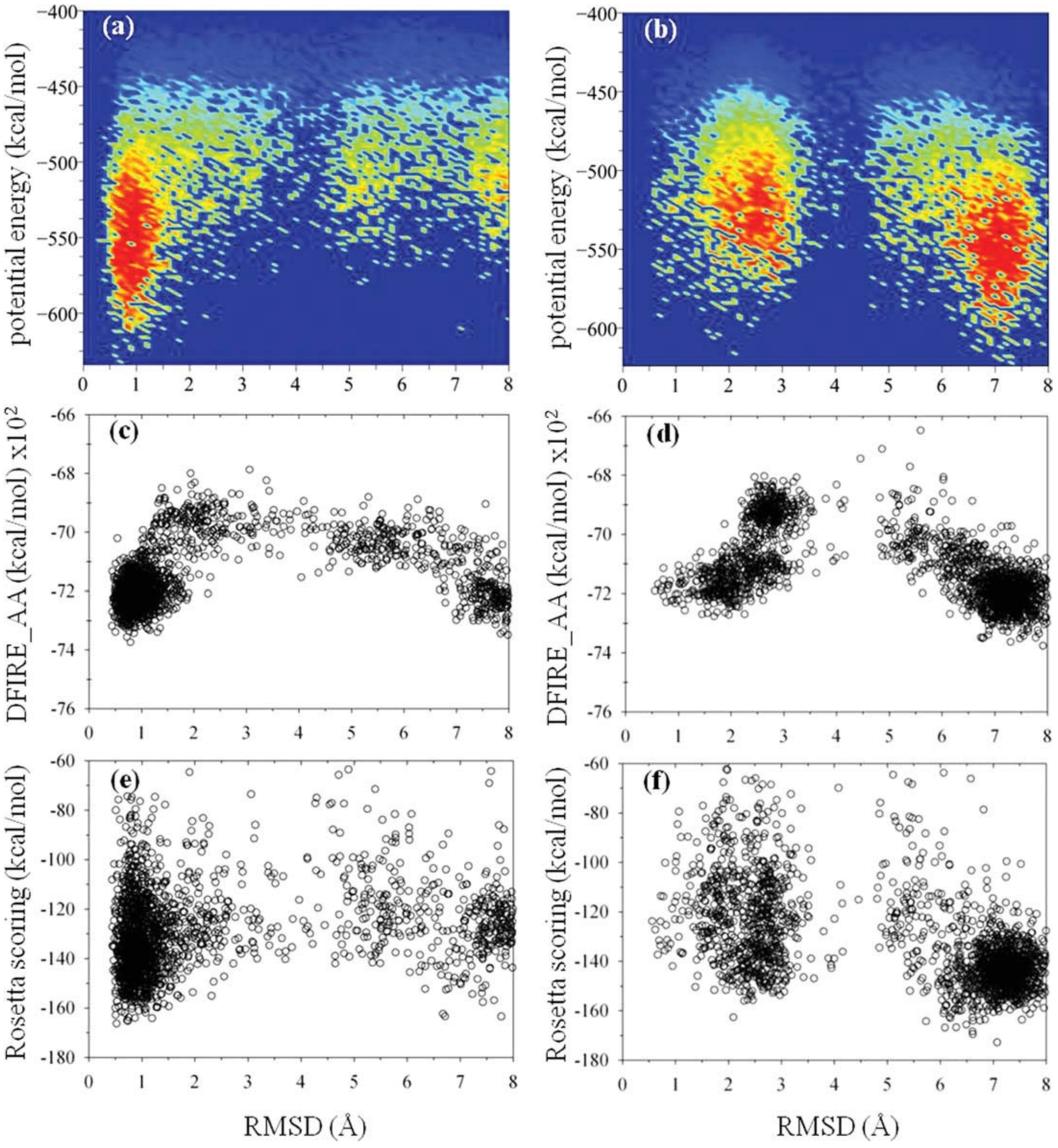

Figure 1. Conformational energy landscape for eight-residue loop target 1plc:6-13 starting from an initial placement of 4.58 Å from the native. a) WHAM profile evaluated at temperature 298 K (red color represents high population density and blue denotes low density). b) WHAM profile for MD simulation. c) DFIRE-AA rescoring of SGLD generated conformations. d) DFIRE-AA rescoring of MD generated conformations. e) Rosetta rescoring of SGLD generated conformations. f) Rosetta rescoring of MD generated conformations.

Evaluation metrics

Both clustering and structure prediction evaluation used the global RMSD of loop backbone atoms between a decoy and a reference structure. This was calculated by superpositioning the backbone atoms of the loop stem residues, defined as residues flanking the loop, of the decoy with that of the reference structure, and then calculating the RMSD between the backbone atoms of the loop residues with those of the reference structure. For hierarchical clustering, the reference structure was another decoy; for evaluating structure predictions, the reference structural was the crystal structure.

Results and Discussion

Table 1 summarizes the simulation results for structure refinement of 8- and 12-residue loops using the two simulation models. All computed RMSD values are for global displacements of the loop backbone coordinates between a predicted structure and the X-ray crystallographic structure. Culled conformations were extracted at a temperature of 298 K and were clustered on the basis of pairwise RMSD distances using a hierarchical clustering scheme.[20,28] Selection of the eight-residue loop targets for assessing the model calculations was taken from previous work,[20] which demonstrated the challenge of all-atom simulations to efficiently populate native basins using the CHARMM22 force field.

Our calculations for the loop targets show the SGLD simulation model to produce more accurate structure refinement than the MD model. For the eight-residue loops, the sampled lowest RMSD conformations calculated by SGLD and MD simulations are roughly comparable in finding nativelike basins; however, SGLD generally performs better in clustering conformers to yield low-RMSD predictions. For the task of

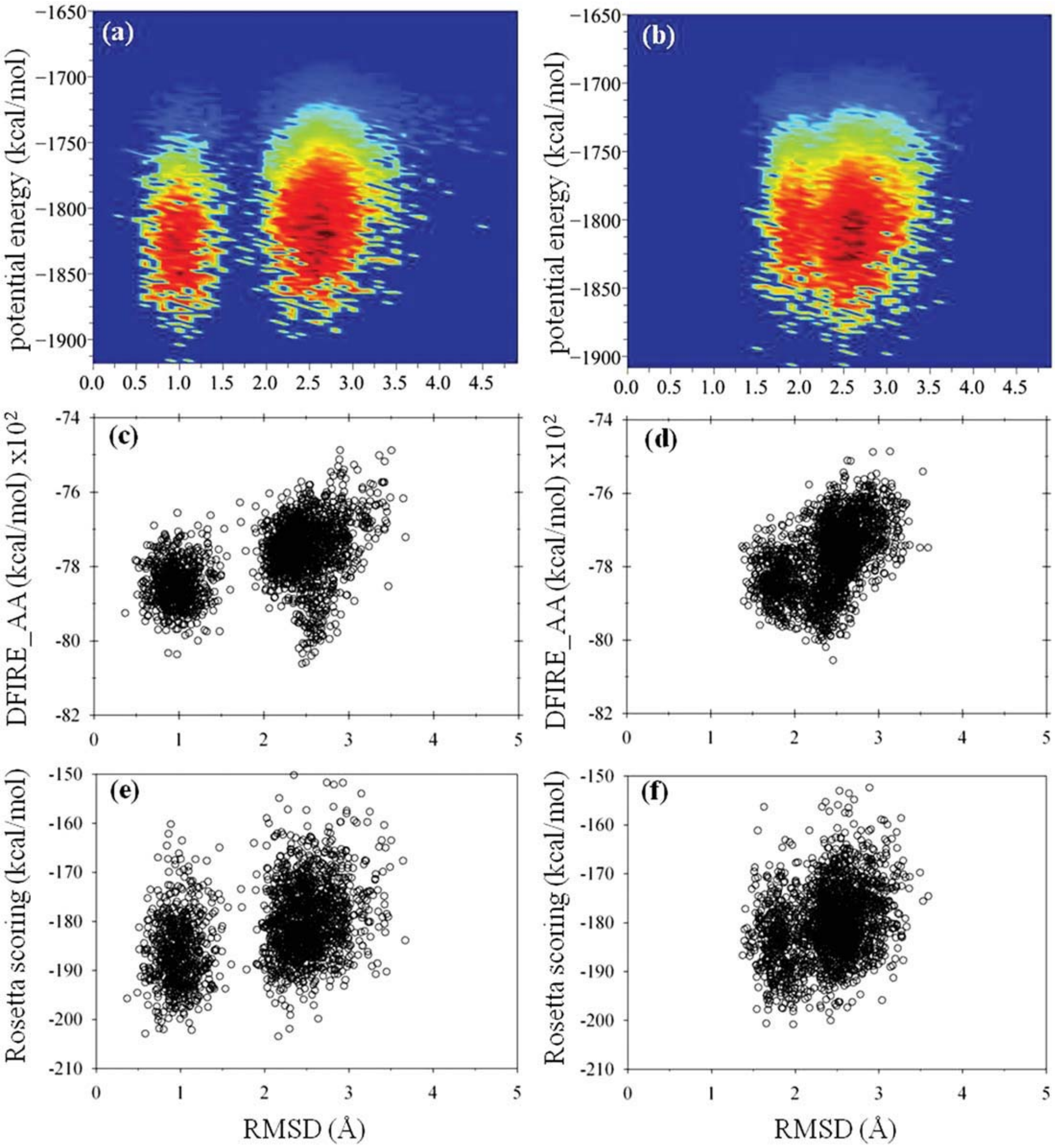

Figure 2. Conformational energy landscape for 12-residue loop target 1bkf:9-20 starting from an initial placement of 2.70 Å from the native. a) WHAM profile evaluated at temperature 298 K for SGLD simulation. Color spectrum similar to that listed in Figure 1. b) WHAM profile for MD simulation. c) DFIRE-AA rescoring of SGLD. d) DFIRE-AA rescoring of MD. e) Rosetta rescoring of SGLD. f) Rosetta rescoring of MD.

detecting nativelike structures, SGLD produces an average RMSD of 0.84 Å across the five targets in the eight-residue loop dataset and MD yields a statistical average RMSD of 2.48 Å, while previously MD using GBMV2 showed 2.56 Å.[20] The GBSW2 provided a better model for populating basins below 2 Å than GBMV2, but both GB models produced largely similar results of detection.

To illustrate the distinction between SGLD and MD for a loop target where the conventional sampling method struggles, Figure 1 shows two-dimensional probability density contour maps of the potential energy versus RMSD at 298 K for protein with PDB ID: 1plc. We define the potential energy as the CHARMM22 + CMAP energy plus the GBSW2 solvent energy. The key observation of the SGLD model is the sharp and narrow cluster of conformers that funnels toward the native basin, yielding structure refinement of an initial 4.6-Å backbone RMSD to a final 0.7-Å conformation. The corresponding MD-computed landscape is strongly bifurcated between near-native (∼2.5-Å RMSD) and non-native loops (∼6–8 Å), with the non-native basin showing greater population density. The comparison between the two models suggests that the guiding force term in SGLD provided an external boost with the net effect of accelerating transitions across a topological barrier at roughly 1.7 Å, whereas traditional MD seems to be locally trapped in less-accurate neighboring basins. Because the potential-energy function is identical for MD and SGLD, the difference in the results of Figure 1 reflects differences in sampling convergence of the two simulation models. Theoretically, executing the MD simulation much longer will eventually produce results similar to SGLD, and thus the latter approach would appear to exhibit a distinct advantage. Below, we highlight individual targets that are representative of the overall results.

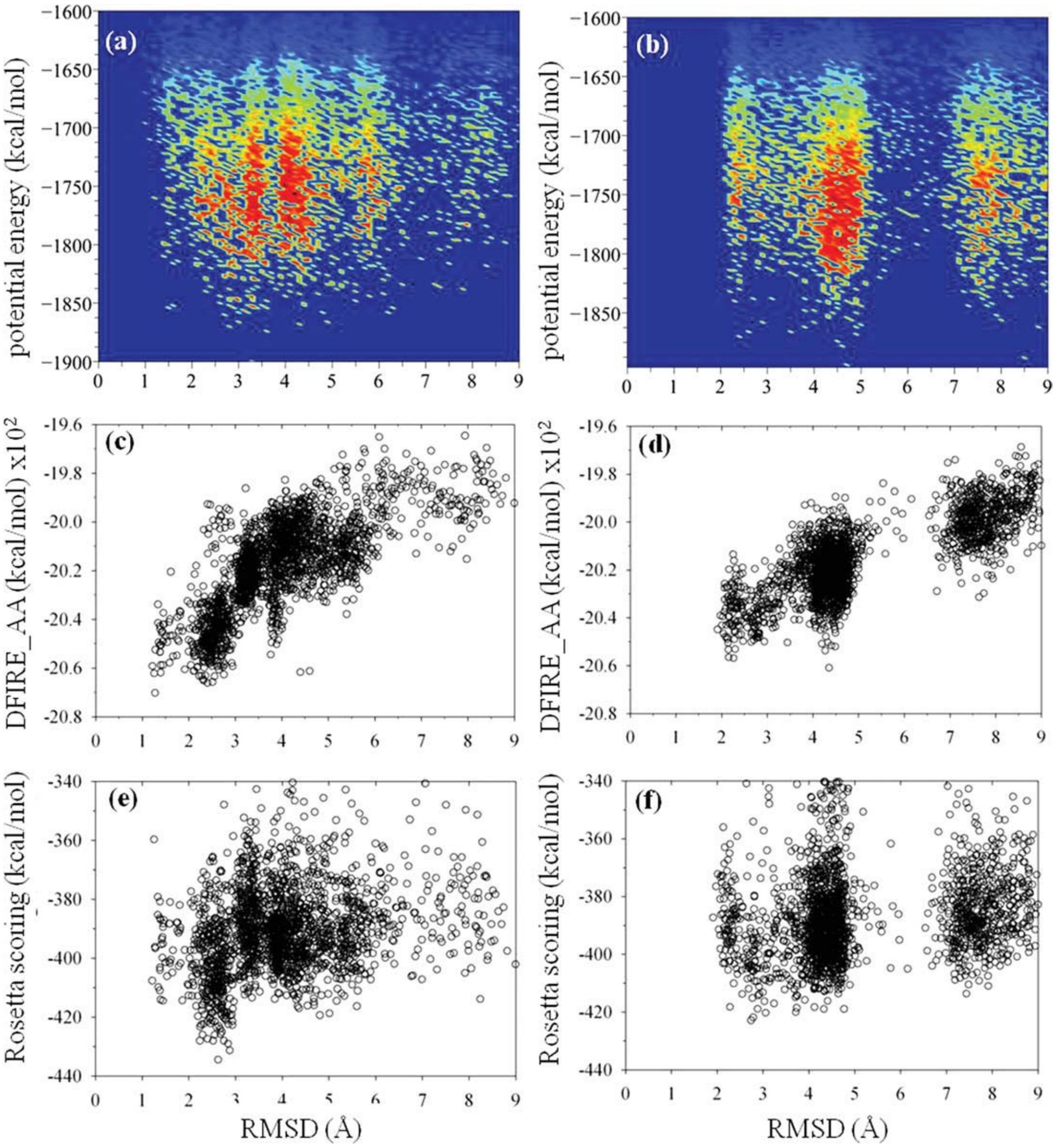

Figure 3. Conformational energy landscape for 12-residue loop target 1ayh:21-32 starting from an initial placement of 4.30 Å from the native. a) WHAM profile evaluated at temperature 298 K for SGLD simulation. Color spectrum similar to that listed in Figure 1. b) WHAM profile for MD simulation. c) DFIRE-AA rescoring of SGLD. d) DFIRE-AA rescoring of MD. e) Rosetta rescoring of SGLD. f) Rosetta rescoring of MD.

For rescoring by the empirical potentials of the lowest temperature replica client conformations generated for eight-residue loop targets, DFIRE-AA yields a statistical average/median RMSD of 1.41/0.63 Å for SGLD and 2.42/0.81 Å for MD. Rosetta produces similar results of 0.83/0.85 Å for SGLD and 2.01/0.78 Å for MD. Figure 1 illustrates DFIRE-AA and Rosetta evaluations of the SGLD and MD models for target 1plc.

Given the promising outcome of refining the eight-residue loops using SGLD simulations, we next evaluate this model for the more difficult 12-residue loops. This small dataset was selected from an earlier reported study of modeling loops using the Protein Local Optimization Program (PLOP).[41] A summary of the results in Table 1 for the 12-residue loop targets shows for SGLD a statistical average/median sampled lowest RMSD basin to be 0.87/0.51 Å and detection to a RMSD of 1.63/0.91 Å. The corresponding MD model results are 1.30/1.27 Å and 2.43/2.22 Å, respectively. For comparison purposes, the average and median starting structure predicted from Loopy is 2.70 Å and the reported PLOP predictions are 2.95/2.99 Å, where in both cases the protein stem of the loop region was modeled as rigid.[30,41] It should be noted that the PLOP method has undergone recent improvements in conformational sampling and detection accuracy applied to different loop target datasets.[41–43] Results for DFIRE-AA are the mean/median values of 1.66/1.62 Å for SGLD and 2.37/2.23 Å for MD, and for Rosetta, the corresponding values are 1.71/1.75 Å for SGLD and 1.88/1.98 Å for MD.

To further demonstrate the comparison between SGLD and MD simulations, we show in Figures 2 and 3 the probability density distribution profiles for loop targets 1bkf and 1ayh.

The outcome from these two loops provides a range of results probably to be observed from modeling a much larger dataset of targets. For 1bkf, the profile computed by MD simulation shows at 2.5–2.8 Å RMSD a large conformational free-energy surface that encompasses the starting structure predicted by Loopy. Budding from this basin is a less-populated cluster near 2 Å. The SGLD simulation produced a similar large basin at 2.6-Å RMSD, yet a nativelike basin emerged near a RMSD value of 1 Å. This result illustrates the enhanced sampling provided by the SGLD model, whereas the MD simulation is principally confined to exploring local regions around the starting loop conformation. Rescoring the conformations by DFIRE-AA show some funnel-like behavior; however, the basin at roughly 2.5 Å is scored too favorably.

In a similar fashion, calculations for 1ayh show the conventional MD method confined mostly to the starting loop conformation at ∼4.5-Å RMSD with some excursions to lower and higher RMSD basins. Unlike the MD model, the SGLD simulations traversed a potential-energy barrier at a RMSD of ∼2 Å. Although both models failed to yield high-resolution refinement, the SGLD model produced an energy landscape that is highlighted by diffusive sampling across multiple major basins. Rescoring the 298 K conformations by DFIRE-AA yields a RMSD funnel for the SGLD model and provides detection to 1.27 Å, whereas rescoring the MD conformers favors the starting basin. On the other hand, Rosetta fails to create funnel shapes for both simulation models and detection is greater than 2 Å.

It is worth noting the energy differences between scoring the X-ray crystallographic structure and the lowest energy conformer for the three scoring approaches. For the comparison, the X-ray structure was subjected to energy minimization using the CHARMM22/GBSW2 force field and then scored for all loop targets. With one exception, alternative conformations generated by the simulations proved to be more favorable when scored by the CHARMM22/GBSW2 model than their corresponding energy-minimized X-ray structures. By contrast, both DFIRE-AA and Rosetta favored the X-ray structures. Although this result is not entirely surprising given the significant parameterization of the empirical models using PDB structures, it does reflect a mismatch of resolution between empirical and physics-based scoring methods. Conformations generated by the simulations were culled from a nonadiabatic excursion of the energy surface and their geometries probably deviate from ideal distributions that empirical functions are parameterized against. Contributing to this is possible artifacts due to the implicit solvent model and having a fixed-charge model rather than a flexible-charge model.[44] It is disappointing that for low-RMSD backbone structures ($<$2 Å) a sharp energy funnel was not created by an approach of repacking the side chains from Rosetta. This result may be attributed, in part, to the resolution of the rotamer library and the lack of energy minimization to effectively redistribute the population landscape.

We conclude that while our benchmark of loop targets is limited, the trend is clear that SGLD provides more accurate structure refinement than traditional MD and achieves a median 1.3-Å resolution increase in the backbone conformation of a starting structure 2.7-Å RMSD from the crystallographic coordinate placement. Given the approximate nature of the guiding force in the SGLD equation of motion and its possible failing of producing a rigorous canonical ensemble,[27] one may have *a priori* anticipated some corruption in the conformational energy distribution in comparison with the MD model using a Nosé–Hoover thermostat. Instead, we found the potential energies from WHAM to be comparable between the two simulation models. Nevertheless, Wu and Brooks have very recently reported a computational strategy to convert a self-guided ensemble to a canonical ensemble, using a reweighting technique.[45] Application of their formulism to complex protein systems await further testing. In this work, the subset of targets with similar outcome provides well-sampled conformational systems where the two sampling methods are proven to converge and thus help validate the SGLD method. Where SGLD excels is enhanced sampling efficiency for loop targets where MD simulations become kinetically trapped. Combining with T-Rex, SGLD offers a better choice for structure refinement of low-resolution models. We also observed no significant advantage to rescoring conformations from the simulations by empirical all-atom energy functions.

Acknowledgments

The authors thank Dr. I-C Yeh and Dr. D. R. Ripoll for valuable discussions. The opinions or assertions contained herein are the private views of the authors and are not to be construed as official or as reflecting the views of the US Army or of the US Department of Defense. This article has been approved for public release with unlimited distribution.

[1] G. Chopra, N. Kalisman, M. Levitt, Proteins 2010, 78, 2668.
[2] G. Chopra, C. M. Summa, M. Levitt, Proc Natl Acad Sci USA 2008, 105, 20239.
[3] C. M. Summa, M. Levitt, Proc Natl Acad Sci USA 2007, 104, 3177.
[4] S. Raman, R. Vernon, J. Thompson, M. Tyka, R. Sadreyev, J. Pei, D. Kim, E. Kellogg, F. DiMaio, O. Lange, L. Kinch, W. Sheffler, B. H. Kim, R. Das, N. V. Grishin, D. Baker, Proteins 2009, 77 (Suppl 9), 89.
[5] P. Bradley, K. M. Misura, D. Baker, Science 2005, 309, 1868.
[6] K. M. Misura, D. Baker, Proteins 2005, 59, 15.
[7] J. Zhu, H. Fan, X. Periole, B. Honig, A. E. Mark, Proteins 2008, 72, 1171.
[8] A. Jagielska, L. Wroblewska, J. Skolnick, Proc Natl Acad Sci USA 2008, 105, 8268.
[9] L. Wroblewska, A. Jagielska, J. Skolnick, Biophys J 2008, 94, 3227.
[10] B. D. Sellers, J. P. Nilmeier, M. P. Jacobson, Proteins 2010, 78, 2490.
[11] J. Chen, C. L. Brooks, III, Proteins 2007, 67, 922.
[12] J. L. MacCallum, L. Hua, M. J. Schnieders, V. S. Pande, M. P. Jacobson, K. A. Dill, Proteins 2009, 77 (Suppl 9), 66.
[13] M. R. Lee, J. Tsai, D. Baker, P. A. Kollman, J Mol Biol 2001, 313, 417.
[14] Y. Sugita, Y. Okamoto, Chem Phys Lett 1999, 314, 141.
[15] X. Wu, B. R. Brooks, Chem Phys Lett 2003, 381, 512.
[16] M. P. Jacobson, D. L. Pincus, C. S. Rapp, T. J. Day, B. Honig, D. E. Shaw, R. A. Friesner, Proteins 2004, 55, 351.
[17] M. S. Lee, M. A. Olson, J Chem Theory Comput 2007, 3, 312.
[18] H. Zhou, Y. Zhou, Protein Sci 2002, 11, 2714.
[19] RosettaCommons, 2010. Available at: http://www.rosettacommons.org. Accessed on April 20, 2010.
[20] M. A. Olson, M. Feig, C. L. Brooks, III, J Comput Chem 2008, 29, 820.
[21] X. Wu, S. Wang, J Chem Phys 1999, 110, 9401.
[22] M. S. Lee, M. A. Olson, J Chem Theory Comput 2010, 6, 2477.
[23] A. D. Mackerell, Jr., D. Bashford, D. M. Bellott, R. L., Dunbrack, Jr., J. D. Evanseck, M. J. Field, S. Fischer, J. Gao, H. Guo, S. Ha, D. Joseph-McCarthy, L. Kuchnir, K. Kuczera, F. T. K. Lau, C. Mattos, S. Michnick, T. Ngo,

D. T. Nguyen, B. Prodhom, I. W. E. Reiher, B. Roux, M. Schlenkrich, J. C. Smith, R. Stote, J. Straub, M. Watanabe, J. Wiorkiewicz-Kuczera, D. Yin, M. Karplus, J Phys Chem B 1998, 102, 3586.

[24] A. D. MacKerell, Jr., M. Feig, C. L. Brooks, III, J Am Chem Soc 2004, 126, 698.

[25] J.-P. Ryckaert, G. Ciccotti, H. J. C. Berendsen, J Comput Phys 1977, 23, 327.

[26] J. Chocholoušová, M. Feig, J Comput Chem 2006, 27, 719.

[27] I. C. Yeh, M. S. Lee, M. A. Olson, J Phys Chem B 2008, 112, 15064.

[28] M. Feig, J. Karanicolas, C. L. Brooks, III, J Mol Graphics Modell 2004, 22, 377.

[29] B. R. Brooks, R. E. Bruccoleri, B. D. Olafson, D. J. States, S. Swaminatham, M. Karplus, J Comput Chem 1983, 4, 187.

[30] Z. Xiang, C. S. Soto, B. Honig, Proc Natl Acad Sci USA 2002, 99, 7432.

[31] E. Gallicchio, M. Andrec, A. K. Felts, R. M. Levy, J Phys Chem B 2005, 109, 6722.

[32] E. Neria, S. Fischer, M. Karplus, J Chem Phys 1996, 105, 1902.

[33] B. Kuhlman, D. Baker, Proc Natl Acad Sci USA 2000, 97, 10383.

[34] R. L. Dunbrack, Jr., F. E. Cohen, Protein Sci 1997, 6, 1661.

[35] B. I. Dahiyat, S. L. Mayo, Science 1997, 278, 82.

[36] J. J. Gray, S. Moughon, C. Wang, O. Schueler-Furman, B. Kuhlman, C. A. Rohl, D. Baker, J Mol Biol 2003, 331, 281.

[37] T. Lazaridis, M. Karplus, Proteins 1999, 35, 133.

[38] A. V. Morozov, T. Kortemme, K. Tsemekhman, D. Baker, Proc Natl Acad Sci USA 2004, 101, 6946.

[39] T. Kortemme, A. V. Morozov, D. Baker, J Mol Biol 2003, 326, 1239.

[40] K. T. Simons, I. Ruczinski, C. Kooperberg, B. A. Fox, C. Bystroff, D. Baker, Proteins 1999, 34, 82.

[41] K. Zhu, D. L. Pincus, S. Zhao, R. A. Friesner, Proteins 2006, 65, 438.

[42] A. K. Felts, E. Gallicchio, D. Chekmarev, K. A. Paris, R. A. Friesner, R. M. Levy, J Chem Theory Comput 2008, 4, 855.

[43] B. D. Sellers, K. Zhu, S. Zhao, R. A. Friesner, M. P. Jacobson, Proteins 2008, 72, 959.

[44] S. Patel, A. D. Mackerell, Jr., C. L. Brooks, III, J Comput Chem 2004, 25, 1504.

[45] X. Wu, B. Brooks, J Chem Phys 2011, 134, 134108.

Received: 16 May 2011,
Accepted: 19 June 2011
Published online on